Remote Sensing in Ecology and Conservation
Open Access
ZSL LET'S WORK FOR WILDLIFE

ORIGINAL RESEARCH

# Synergetic use of Sentinel-1 and Sentinel-2 for assessments of heathland conservation status

Johannes Schmidt[1], Fabian E. Fassnacht[1], Michael Förster[2] & Sebastian Schmidtlein[1]

[1]Institute of Geography and Geoecology, Karlsruhe Institute of Technology, Karlsruhe D-76131, Germany
[2]Geoinformation in Environmental Planning Lab, Technical University of Berlin, BerlinD-10623, Germany

**Keywords**
*Calluna vulgaris*, habitats directive, monitoring, Natura 2000, SAR, spaceborne remote sensing

**Correspondence**
Johannes Schmidt, Institute of Geography and Geoecology, Karlsruhe Institute of Technology, D-76131 Karlsruhe, Germany.
Tel: +49 721 60844367; Fax: +49 721 60843738;
E-mail: johannes.schmidt@kit.edu

**Funding Information**
The study was supported by the German Federal Environmental Foundation (DBU, www.dbu.de).

Editor: Harini Nagendra
Associate Editor: Clement Atzberger

Received: 11 July 2017; Revised: 16 October 2017; Accepted: 20 October 2017

doi: 10.1002/rse2.68

*Remote Sensing in Ecology and Conservation* 2018;**4** (3):225–239

## Abstract

Habitat quality assessments often demand wall-to-wall information about the state of vegetation. Remote sensing can provide this information by capturing optical and structural attributes of plant communities. Although active and passive remote sensing approaches are considered as complementary techniques, they have been rarely combined for conservation mapping. Here, we combined spaceborne multispectral Sentinel-2 and Sentinel-1 SAR data for a remote sensing-based habitat quality assessment of dwarf shrub heathland, which was inspired by nature conservation field guidelines. Therefore, three earlier proposed quality layers representing (1) the coverage of the key dwarf shrub species, (2) stand structural diversity and (3) an index reflecting co-occurring vegetation were mapped via linking *in situ* data and remote sensing imagery. These layers were combined in an RGB-representation depicting varying stand attributes, which afterwards allowed for a rule-based derivation of pixel-wise habitat quality classes. The links between field observations and remote sensing data reached correlations between 0.70 and 0.94 for modeling the single quality layers. The spatial patterns shown in the quality layers and the map of discrete quality classes were in line with the field observations. The remote sensing-based mapping of heathland conservation status showed an overall agreement of 76% with field data. Transferring the approach in time (applying a second set of Sentinel-1 and -2 data) caused a decrease in accuracy to 73%. Our findings suggest that Sentinel-1 SAR contains information about vegetation structure that is complimentary to optical data and therefore relevant for nature conservation. While we think that rule-based approaches for quality assessments offer the possibility for gaining acceptance in both communities applied conservation and remote sensing, there is still need for developing more robust and transferable methods.

## Introduction

Central European lowland heathlands occur largely as a replacement-vegetation of forests triggered by past land-use and current conservation management. These heathlands are characterized by a low woody vegetation layer that is typically formed by a single ericaceous species, *Calluna vulgaris* (L.) Hull, interspersed by open soil and sparse vegetation. Most *Calluna* shrublands are of conservation interest and protected within the Natura 2000 conservation network, which requires periodic monitoring reports about the habitats' state.

As demonstrated in earlier studies, remote sensing can be a potentially useful tool to support such monitoring tasks (e.g. Bock et al. 2005; Förster et al. 2008; Vanden Borre et al. 2011). Most earlier studies used only passively recorded optical imagery while only few studies in the field supplemented optical information with data from active sensors like LiDAR (e.g. Leutner et al. 2012; Kepfer-Rojas et al. 2015; Zlinszky et al. 2015) and synthetic aperture radar (SAR). LiDAR and SAR data are complementary to optical sensors, as their measurements mostly relate to the physical structure of the vegetation which is only partly described by the optical signal.

Only few studies have examined SAR data for mapping purposes in dwarf shrub heathlands or herbaceous vegetation. These studies include an analysis of time series of TerraSAR-X backscatter information to detect swath events in grasslands (Schuster et al. 2011) as well as for the differentiation of grassland types (Schuster et al. 2015). Very accurate classifications between grassland and crops were reported by Dusseux et al. (2014) when using multitemporal optical imagery and polarimetric SAR products in combination. Bargiel (2013) achieved high accuracies for classifying vegetation types, such as shrub patches and grassland based on a multichannel TerraSAR-X time series. SAR time series from ERS-2 and ASAR enabled Millin-Chalabi et al. (2013) to detect a fire scar in a upland moorland. To obtain information on shrub growth in the Sub-Artic, Duguay et al. (2015) applied TerraSAR-X and Radarsat-2 in combination with *in situ* data. They compared the backscatter signal of both sensors concerning their sensibility for detecting shrub density and height.

Fusing actively and passively sensed data provides information about both the structure and the material content of the depicted objects. The synergistic use of SAR and optical remote sensing was applied in several studies for describing vegetation in diverse ecosystems, for example, forests (Montesano et al. 2013; Reiche et al. 2015), wetlands (Rodrigues and Souza-Filho 2011; Hong et al. 2015), agricultural areas (Hill et al. 2005; Peters et al. 2011), upland vegetation types (Barrett et al. 2016) and also to differentiate broad land cover classes (Ullmann et al. 2014). However, up to now, there are no studies attempting to exploit SAR-optical synergies for mapping and characterizing conservation areas.

Although several studies have been dealing with the development of remote sensing-based approaches for the European monitoring procedures of the Natura 2000 framework (see Corbane et al. 2015 for a synthesis), these methods are still not widely applied in an operational context. One reason for this might have been the lack of suitable, operational datasets. European Union's new sensor systems Sentinel-1 (S1) and Sentinel-2 (S2) might help to increase the applicability of remote sensing-based procedures in practical monitoring tasks. There have already been vegetation-focused studies using Sentinel data (e.g. Immitzer et al. 2016; Clevers et al. 2017; Delgado-Aguilar et al. 2017), but there is no work directly dealing with conservation mapping based on Sentinel data, even though Feilhauer et al. (2014) proved S2 imagery to be potentially useful for Natura 2000 monitoring when applying simulated data.

In our study, we jointly analyze multispectral Sentinel-2 and Sentinel-1 SAR data of EU's Copernicus mission for habitat mapping and monitoring purposes. For an example of dwarf shrub heathland habitats, we use combined SAR multispectral datasets to create a habitat map that suits the monitoring demands of the European Habitat Directive. To achieve that, we adapt an approach proposed by Schmidt et al. (2017b) who transferred field mapping guidelines to a remote sensing approach. This earlier approach bases on remote sensing proxies from airborne data reflecting wall-to-wall information on (1) the key species, (2) stand structural diversity and (3) co-occurring vegetation. Here, we combine spaceborne remote sensing data and field samples to obtain the same three variables and finally derive spatial representations of continuous habitat states and discrete conservation status classes.

## Materials and Methods

### Study area and occurring habitats

The study was conducted in the Oranienbaum Heath located near Dessau, Saxony-Anhalt, Germany (N 51.77350°, E 12.36120°; Fig. 1). For a detailed description of the study area see Schmidt et al. (2017a).

The dominant communities of the non-forested areas in the study include dwarf shrub associations (Natura 2000 habitat types H-2310 and H-4030) characterized by high coverages of *Calluna vulgaris* (henceforth simply *Calluna*). These habitats are characterized by the aging-cycle of *Calluna* where the plants undergo a cyclic succession of different phases, each with a characteristic species composition (Watt 1947; Gimingham 1972). In terms of conservation, heathland patches in optimal states feature mosaics of these phases being interspersed by cryptogams and sparse grassland (Ausden 2007).

Besides the dwarf shrub habitats, grassland occurs in varying forms. Open pioneer grasslands (H-2330 with *Corynephorus* and *Agrostis*) appear on inland dunes. Calcareous sandy grasslands (H-6120) mainly occur in the south of the study area and are featuring a high species diversity. They are often neighboring other low-nutrient grasslands or *Calluna* heath patches, thereby forming a mosaicked vegetation. Heathland degraded by grass encroachment of *Calamagrostis epigejos* can mainly be found in the northern and central part.

### Data

#### Vegetation assessments in the field

Three field datasets were used for calculating the quality layers that provide the basis for an integrated assessment of habitat quality (Fig. 2). Coverage ratios of vascular plants were recorded in 85 plots measuring 10 × 10 m in

 

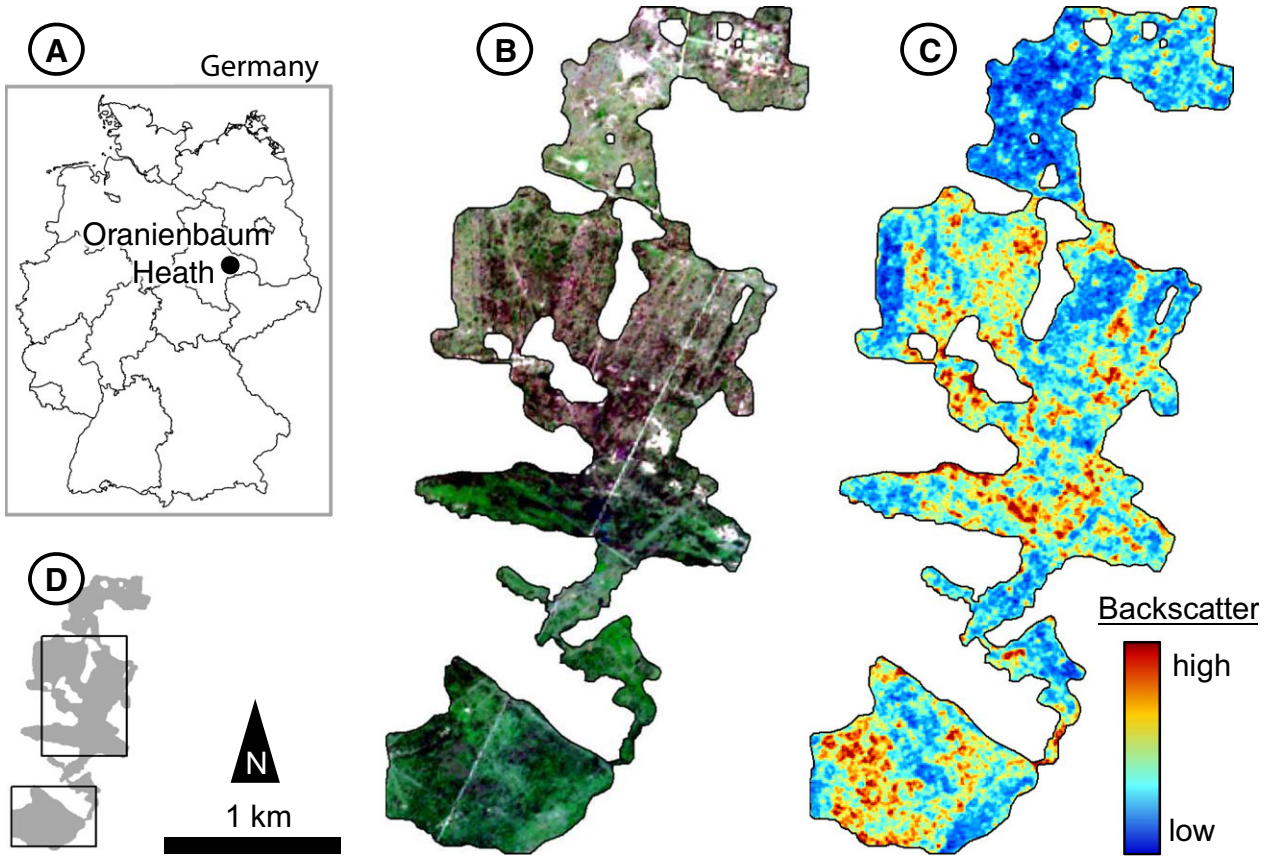


**Figure 1.** The study site Oranienbaum Heath is located near Dessau, Saxony-Anhalt, Germany (A). Panel B gives an impression of the multispectral data used in this study (Sentinel-2; RGB-bands: 4, 3, 2). Forests are masked. SAR backscatter information from Sentinel-1 provided information on the vegetation structure (C; mean of ascending and descending VH backscatter). As the target habitat *Calluna* heathland is mainly found in the central and southern part of the study, we focus on these areas when mapping the habitat quality (D).

August 2014. The samples were located in the field with a stratified random approach using an earlier mapping by Felinks et al. (2012) to ensure that all occurring heathland habitats were considered. In the following, we will refer to this dataset as 'species dataset'. These plots served as basis for calculating a species index as described below and for validating the habitat mask.

Coverage values of *Calluna* were documented for 400 plots measuring 10 × 10 m in July 2015 ('*Calluna* dataset'). In 160 of these samples, we additionally sampled mean height and standard deviation of the height from 15 measurements of the vegetation height within the sample plot ('structure dataset'). The plot locations were chosen by stratified random samplings based on the habitat map from Schmidt et al. (2017b) to ensure that the target habitat is captured in all its specificities.

Independent from that, another field mapping was conducted in July 2015 where 350 plots measuring 10 by 10 m that represent *Calluna* habitats were checked for their conservation status ('conservation status dataset'). This dataset was split into a training and a validation dataset (50/50) based on stratified random sampling. The training set was used for calibrating the rule-based decision tree, while the validation set served as basis for validating the resulting conservation status classification.

## SAR data

Sentinel-1 (S1) is a dual polarization radar (VV and VH) that measures two-dimensional surface backscattering using a C-band SAR with 6 cm wavelength (ESA, 2016a). Being a short wavelength SAR, the signal of Sentinel-1 interacts with the upper part of vegetation canopies allowing for retrieving biophysical vegetation parameters.

We acquired level-1 products (*Ground Range Detected with high resolution*) from the end of June / beginning of July, recorded in *interferometric wide swath* mode. The processing of the SAR imagery in SNAP (ESA, 2016c)

 

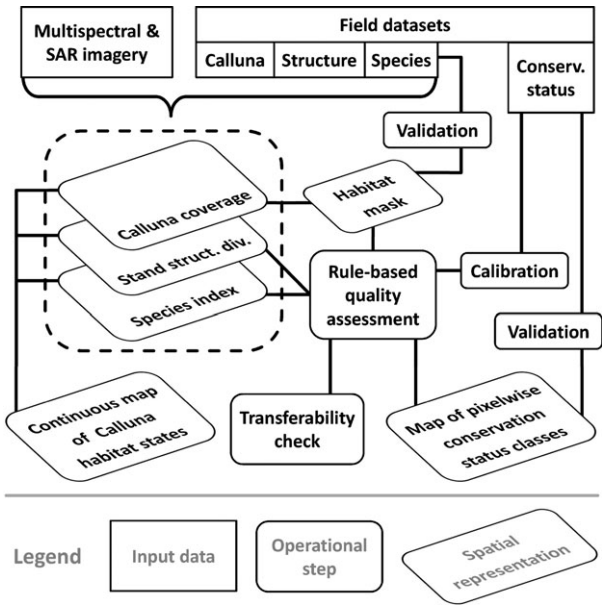


**Figure 2.** Workflow of the study. We created three independent models representing the quality layers named (1) *Calluna* coverage (using both multispectral and SAR data), (2) stand structural diversity (using SAR) and (3) a species index (using multispectral imagery). The three spatial layers were used for a continuous graphical representation of the three quality layers determining the habitat conservation status. Afterwards, the actual conservation status classes were derived by rule-based classification conducted on pixel-level.

included the application of an orbit file, geometric calibration, terrain correction and speckle filtering. As it has been shown in other applications that a fusion of ascending and descending SAR data can minimize geometric distortions (e.g. Goering et al. 1995 for noise removal; Gernhardt and Bamler 2012 for detecting building deformation; Deo et al. 2015 for DEM generation), we applied scenes that were acquired in two different orbits (Table 1). Additionally, we fused the SAR images by applying an weighted average approach (Carrasco et al. 1997; Sansosti et al. 1999; Crosetto 2002).

The six bands (VV and VH for two passes plus the respective means) were merged in a stack featuring a spatial resolution of 10 m. In addition, we calculated the

**Table 1.** Satellite data used in this study.

| Dataset | Sensor | Date | DOY | Pass |
|---|---|---|---|---|
| Calibration | S2 | 2016-06-28 | 180 | D |
| | S1 | 2016-06-30 | 182 | A |
| | | 2016-07-09 | 191 | D |
| Transfer | S2 | 2016-06-08 | 160 | D |
| | S1 | 2016-06-08 | 160 | D |
| | | 2016-06-11 | 163 | A |

S2: Sentinel-2, S1: Sentinel-1, D: descending orbit, A: ascending orbit.

textural features *variance* and *entropy* in R (package *glcm*; Zvoleff 2015) based on 3 × 3 gray-level co-occurrence matrices (Haralick et al. 1973) for each band but the mean layers. The SAR imagery served as basis for creating a threshold-based forest mask where the threshold was identified by visual interpretation.

In order to check for transferability, the classification procedure was also conducted on a second set of SAR images that were acquired around 25 days before the calibration image set (Table 1).

### Multispectral imagery

As multispectral dataset, we applied a Sentinel-2 (S2) (ESA, 2016b) image that was acquired on 28th of June 2016. We used the ten bands with 10 and 20 m spatial resolution that cover the spectrum from 490 nm to 2190 nm, scaling those with 20 m pixels down to 10 m. The original S2 data were re-projected and processed using SNAP. The textural feature *contrast* was calculated and, finally, the SAR-based forest mark was applied.

The transferability check was performed based on a second multispectral image, which was acquired 20 days before the calibration image (Table 1).

## Methods

### Transfer of the field guidelines to remote sensing

According to the regional mapping guidelines (LAU, 2010), the habitat status of *Calluna* areas should be described based on three criteria: a primary requirement of an area to qualify as *Calluna* habitat is a minimum coverage of the key species *Calluna* of 30%. Furthermore, the occurrence of different successional phases of *Calluna* at short distance is considered to indicate a favorable conservation status. This situation can be described with a high structural diversity. A further indicator for a high conservation quality class are sparse grasslands as co-occurring vegetation. Hence, species typically found in sparse grasslands are listed as indicators of favorable habitat conditions. They include, for example, *Anthoxanthum odoratum*, *Festuca ovina*, *Koeleria macrantha*, *Rumex acetosella* and *Thymus pulegioides*. Negative habitat pressure is represented by bush or grass encroachment as well as the occurrence of neophytes or species indicating eutrophication. According to the field guidelines, these three criteria should be assessed in the field and summarized in a categorical vote including the classes "favorable" (A), "inadequate" (B) or "bad" (C), that is, the conservation status.

These guidelines for mapping *Calluna* habitats in the field were transferred to a remote sensing approach by Schmidt et al. (2017b) who proposed to approximate the

 

field mapping parameters by three remote sensing proxies (quality layers): (1) coverage of the key species *Calluna*, (2) stand structural diversity and (3) a species index reflecting co-occurring vegetation. All information that is needed for assigning the conservation status is potentially captured either by a single remote sensing-based quality layer or a combination of several of them.

In this remote sensing approach, a continuous layer representing cover ratios of *Calluna* (*Calluna* cover per pixel) serves to create a mask of the target habitat by excluding areas that do not have an appropriate fraction of *Calluna* cover (<30%) and therefore do not qualify as target habitat. Afterward, wall-to-wall information about stand structure and vegetation co-occurring with *Calluna* is used for discriminating the quality classes within the remaining areas. Mean canopy height is combined with the standard deviation in order to jointly represent stand structural diversity. A species index proposed by Schmidt et al. (2017b) is then used to describe the vegetation that co-occurs with *Calluna*. The index is defined as a simple ratio between the coverage of indicator species for "favorable" and "bad" conservation status: $i = n_f \log (c_f)$-$n_b \log (c_b)$; where $n_f$ and $c_f$ are the number and the cover species indicating a "favorable" status, while $n_b$ and $c_b$ are the corresponding values of species indicating a "bad" status. Standardization is achieved by dividing the index by its maximum value.

By applying thresholds based on expert judgment to the modeled quality layers, the final categorical status classes are derived. This map depicting the pixel-wise conservation status was then compared to mapping results from an independent field dataset. This procedure is following the principle proposed by Regan et al. (2004) who suggested to formalize experts' decision making processes as common in the conservation status assessment under the Habitats Directive, in order to transfer the rules to remote sensing products. We assume the concept to be transferable to shrublands that have similar characteristics. Technical descriptions how the remote sensing proxies were calculated follow below.

## Model building

We applied Support Vector Machines (SVM) regressions to obtain all three quality layers. We selected SVM as a nowadays conventional method for treating higher dimensional remote sensing data (i.a. Fassnacht et al. 2014; Mack et al. 2016; Schuster et al. 2015). A good description of SVM in the context of remote sensing is given by Mountrakis et al. (2011).

We applied SVM regression with a radial basis function kernel based on the R package *kernlab* (Karatzoglou et al. 2004). The SVM applications were performed in *R* (R Development Core Team, 2013) using the *caret* package (Kuhn 2016). The tuning parameters sigma and cost were kept constantly with 0.1 and 1, respectively. The model fits of SVM are reported in $R^2$, root-mean-square deviation (RMSD), and normalized root-mean-square error (nRMSE) as obtained by 10-fold cross-validation with 30 repeats. A normalized RMSE allows for comparisons between the models as the result is dimensionless (expressed in percentage). Following Piñeiro et al. (2008), we also documented intercept and slope of a linear model between observed and predicted values as well as the results of testing the equality to 0 (intercept) and 1 (slope), respectively, based on regression scatter plots of observed versus predicted values (OP). The influence of the different input variables on model performance was assessed via variable importance evaluation.

For creating the habitat mask, *Calluna* coverages were calculated by regressing coverage values of the *Calluna* dataset ($n = 400$) against fused SAR and multispectral data. As stand structure is represented by both canopy height and its diversity, we calculated two SVM models based on the 160 field samples of the structure dataset. The mean of 15 values per field sample was considered for modeling the mean canopy height, whereas standard deviation was considered for modeling the height diversity. Combining these two spatial representations helped to separate areas that feature a similar canopy height but differ in their structural diversity, as well as the other way around. Furthermore, the key species index reference values (species dataset, $n = 85$) were regressed against the S2 multispectral imagery to achieve information about the co-occurring vegetation for the whole study area.

## Creating the habitat mask

For the designation of the target habitat, only pixels with more than 30% *Calluna* coverage were considered. To ensure that fringes of *Calluna* heathland habitats are included in the evaluation (like in field mapping), the mask was slightly smoothed by applying a mean filter ($3 \times 3$). For validating this remote sensing-derived habitat mask, we compared it with field-based vegetation clusters from the species dataset. The isopam algorithm (Schmidtlein et al. 2010) was used to differentiate vegetation into four types: *Calluna* heathland, calcareous sandy grassland, open sandy grassland and degraded heathland dominated by *Calamagrostis epigejos*. The three clusters that are not associated with *Calluna* heathland were merged. Here, 76 out of 85 plots were considered; nine were masked due to the application of the forest mask.

 

### Visualizing *Calluna* habitat states and deriving the conservation status

To depict the final habitat status of the heathlands, we followed two approaches: On the one hand, we combined the single quality layers in a Red-Green-Blue (RGB) color composite map. Within this RGB map, the coverage of *Calluna* is represented in red, stand structural diversity in green and the species index in blue. Stand structural diversity is represented by the coefficient of variation between the standard deviation and the mean vegetation height. This map illustrates the variety of habitat states as gradients in the landscape.

On the other hand, discrete quality classes were derived in a procedure very similar to the field assessment. The coverage of *Calluna* was only crucial for identifying the habitat type, not for assessing the habitat quality. Then co-occurring vegetation and stand structural diversity served as parameters in a decision tree approach (Fig. 3). The thresholds were approached by gradually changing the values in order to achieve the highest possible agreement between the field data (training set) and the remote sensing result; the fit was assessed by a confusion matrix (using the validation set). We intentionally name that step "comparison" (resulting in a "fit" instead of "accuracy") as we assume that it is rather a matching test than validating a dataset with a true reference dataset (Foody 2008; and further discussed in Schmidt et al. 2017b).

### Transferability check

In order to test the transferability of the proposed method and to assess the influence of short-term variation in image attributes and weather on the results, we transferred the workflow to another remote sensing dataset acquired around 3 weeks before.

## Results

### Modeling results

Modeling the *Calluna* coverage resulted in an $R^2$ of 0.94 and a RMSD of 13.92 (Fig. 4A, Table 2). The obtained %cover values varied between −6% and 97%. Values below 0 occurred in large sandy areas with high reflectance values. Judging from the SVM predictor importance measure, multispectral bands (especially from the visible region as well as the beginning of red edge and SWIR) were important for the SVM regression, whereas the associated contrast-textures were not meaningful (see Table S1 for variable importance results of all SVM regression models). Three SAR-bands were prominent: VH of the descending pass, the mean VH-band, and the ascending VV texture *variance*.

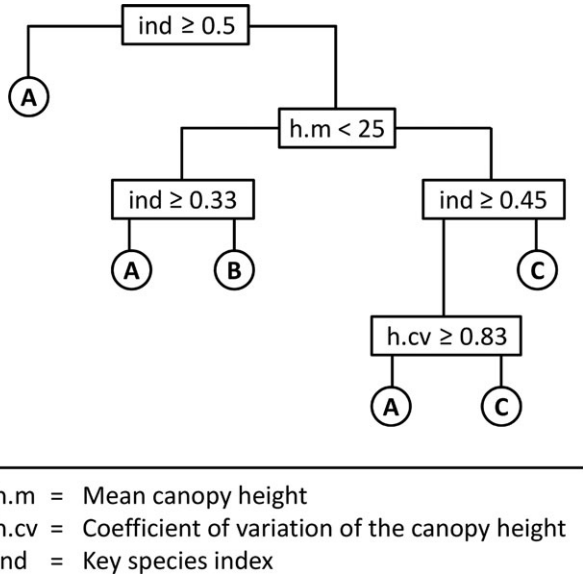


**Figure 3.** Rule-based decision tree for separating the three conservation status classes based on the mean vegetation height, coefficient of variation of the height and the species index. The latter was particularly important for separating quality class 'A' from both 'B' and 'C'. Classes 'B' and 'C' could be well distinguished based on the mean height. The coefficient of variation of the vegetation height was useful for minor adaptions.

The models for canopy height (mean height and standard deviation) reached $R^2$s of 0.71 (RMSD = 8.49) and 0.70 (6.0), respectively (Fig. 4B and C). Highest mean canopy height of around 40 cm was predicted for the dense *Calluna* stands, lowest was found in light meadows and open sandy sites (ca. 7 cm). High structural diversity (standard deviation of vegetation height) with values above 25 was found for edge regions of dense *Calluna* patches as well as for the mosaicked vegetation of shrubs and grassland. Grassland generally featured low values around 10. Although the importance-scores varied for both models, the mean VH-band and the *variance*-textures of ascending VH and VV were comparably important.

The spatial representation of co-occurring vegetation is based on a model with an $R^2$ of 0.77 and a RMSD of 0.2 (Fig. 4D). The sparse calcareous meadows in the Southeast of the study area show highest species index values of up to 0.95. Lowest values around 0.1 can be observed in areas featuring severe grass encroachment. Two bands in the red edge (740, 783 nm) showed high importance values in this model.

The model outcomes of the transfer remote sensing dataset were similar to the reference dataset. The model results for both remote sensing datasets are summarized in Table 2.

 

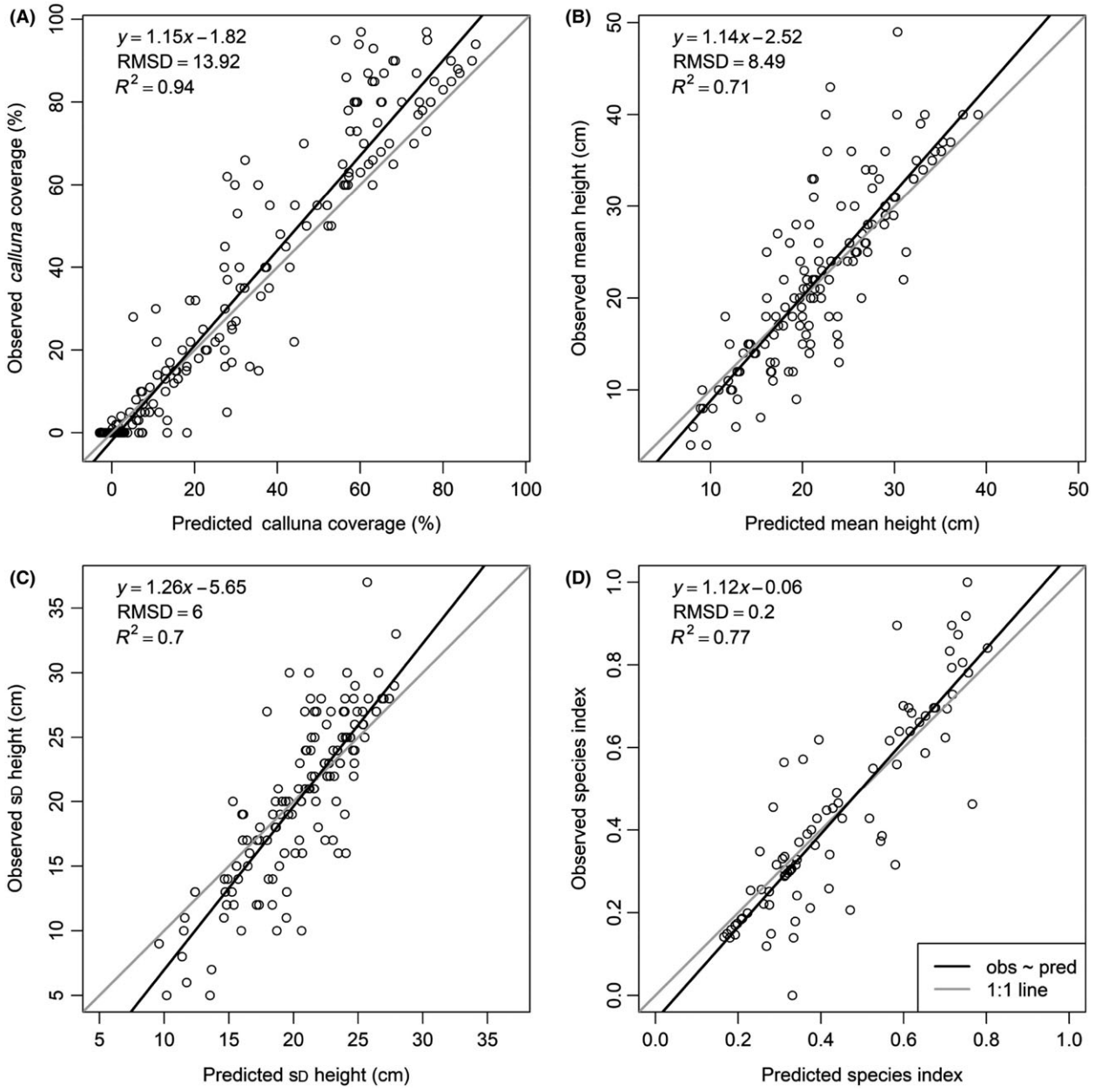


**Figure 4.** Scatterplots between observed and predicted values of the four SVM models. An overestimation of the extreme values can be observed for modeling *Calluna* coverages (A), whereas for the height models (B, C) extreme values seem to be rather underestimated.

## Habitat mask, habitat state and conservation status

The habitat mask enabled us to separate *Calluna* heathland from the other habitats with an accuracy of 84% (Kappa = 0.63). *Calluna* heathland covered an area of 158 ha (33% of the study area). As 34 plots of the test dataset were found to be outside the habitat mask, we proceeded with 316 reference plots for assessing the fit of the conservation status mapping.

The three quality layers *Calluna* coverage (R), structural diversity (G) and key species index (B) span the RGB color space in Figure 5A. This continuous map reveals gradients of habitat states described by different stand attributes. This continuous illustration was not validated in a statistical manner, but examined visually. The displayed spatial patterns of varying *Calluna* habitat states predominantly agreed to what was expected from fieldwork.

Concerning the derived conservation status classes (Fig. 5B), we found that tall and less-structured vegetation

 

**Table 2.** (A) Regression results (SVM) for the single quality layers for the calibration imagery from the end of June / beginning of July. (B) Regression results (SVM) for the single quality layers for the transfer imagery from beginning of June.

| Product | RS data | Ref. (*n*) | Pred. (*n*) | $R^2$ | RMSD | nRMSE (%) | Interc. | Sign. (*b* = 0) | Slope | Sign. (*a* = 1) |
|---|---|---|---|---|---|---|---|---|---|---|
| (A) | | | | | | | | | | |
| *Calluna* cover | Multisp. & SAR | 400 | 34 | 0.94 | 13.92 | 8.3 | −1.82 | <0.001 | 1.15 | <0.001 |
| Mean height | SAR | 160 | 14 | 0.71 | 8.49 | 10.9 | −2.52 | 0.057 | 1.14 | <0.001 |
| SD height | SAR | 160 | 14 | 0.70 | 6.00 | 10.8 | −5.65 | <0.001 | 1.26 | <0.001 |
| Key Species | Multisp. | 85 | 20 | 0.77 | 0.20 | 11.4 | −0.06 | 0.068 | 1.12 | <0.001 |
| (B) | | | | | | | | | | |
| *Calluna* cover | Multisp. & SAR | 400 | 34 | 0.95 | 13.11 | 7.8 | −1.35 | 0.001 | 1.13 | <0.001 |
| Mean height | SAR | 160 | 14 | 0.71 | 8.68 | 11.1 | −3.16 | 0.023 | 1.17 | <0.001 |
| SD height | SAR | 160 | 14 | 0.60 | 6.69 | 12.1 | −2.97 | 0.061 | 1.14 | <0.001 |
| Key Species | Multisp. | 85 | 20 | 0.76 | 0.20 | 11.7 | −0.05 | 0.126 | 1.11 | <0.001 |

with the absence of characteristic co-occurring species leads to a 'C'-assignment ("bad" conservation status, 37% of the habitat). This is mostly the case for old, dense *Calluna* stands. Areas that show rather low values for the species index, but feature a more diverse stand structure are considered as "inadequate" ('B', 29%). The situation mostly occurred in moderately degraded heathland, where grass encroachment already suppresses the occurrence of low-growing grasses and herbs. Class 'A' ("favorable", 34%) is found when there is a high score of characteristic co-occurring vegetation, expressed by a medium to high species index. In an ideal case, this coincides with a heterogeneous stand structure; a case that is often found in peripheral zones of dense *Calluna* stands. Summarized, *Calluna* habitats in the southern part of the study area are mainly in a "favorable" status (due to favorable co-occurring vegetation according to the nature conservation guidelines) except for some patches of overaged heather. This classification result was compared with the field estimates from the validation dataset ($n$ = 158) resulting in an overall fit of 76% and a Kappa of 0.64 (Table 3).

By transferring the procedure to a second remote sensing dataset from beginning of June, another set of quality layers could be obtained with comparable correlations (Table 2). Applying the decision tree with the same parameters resulted in a fit of 73% (Kappa = 0.60) in comparison to the field samples. It can be seen from Fig. 6 that the general patterns of conservation status classes are similar between both datasets. Problematic differences between the two maps (switch from 'C' to 'A') are observable in the upper part of the northern subarea.

## Discussion

The aim of this study was to derive conservation status classes of dwarf shrub heathland using remotely sensed habitat quality layers (describing vegetation properties) and a rule-based classification procedure. Continuous quality layers were obtained from regressing *in situ* data against spaceborne multispectral Sentinel-2 and Sentinel-1 SAR imagery. The single quality layers on their own provide useful information for ecologists and site managers; in combination they reveal a variety of stand attributes describing habitat states in a spatially continuous way. This allows for detecting transitions and gradients that are not apparent in patch-wise conservation status representations as required by reports according to the European Flora Fauna Habitat convention. The procedure allows after-the-fact revisions of thresholds used to define the conservation status which is hardly possible with field-based assessments.

The overall fit of 76% in the estimation of conservation status classes was comparably high regarding the result of 65% achieved by Schmidt et al. (2017b) following a similar procedure based on airborne hyperspectral remote sensing. This is remarkable, as only ten S2 bands were used in this study in contrast to the hyperspectral AISA-sensor applied in Schmidt et al. (2017b). This confirms earlier reported observations concerning the high potential of the S2 bands for efficient vegetation analyses (Clasen et al. 2015).

### Contribution of the single quality layers

The derived quality layers showed limitations in some parts of the study area. For example, we encountered problems in areas with low *Calluna* coverages. Some pixels with no or very low *Calluna* coverage values were predicted to have coverages of up to 20%. It is likely, that at very low *Calluna* coverages the contribution of the *Calluna* vegetation to the observed spectral signal is too low to build robust model. Furthermore, overexposure effects caused by areas with high amounts of sand or litter (Nagler et al. 2000) presumably contributed to the reduced performance of the regression models in these areas. On the contrary, *Calluna* coverages above 25% were slightly underpredicted. Other approaches such as spectral unmixing (Delalieux et al.

 

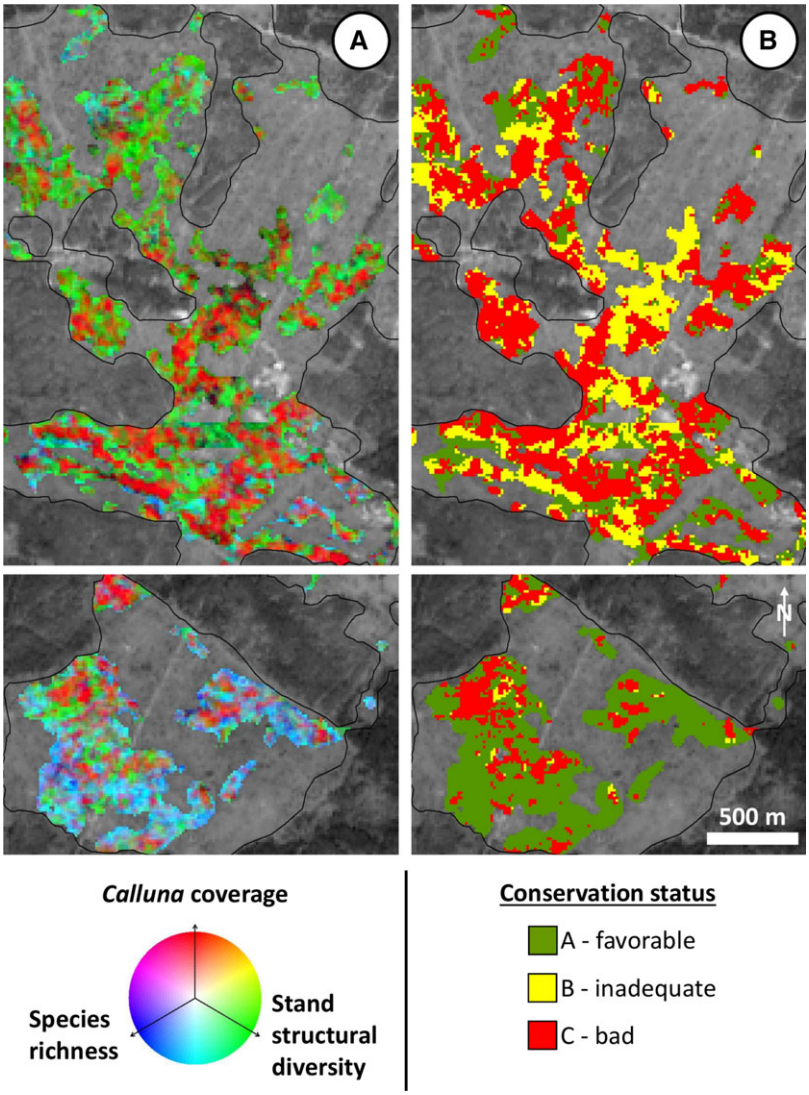


**Figure 5.** The habitat state of *Calluna* heathland is visualized via an RGB-representation (A) in two subareas of the study site (Fig. 1D). A habitat mask was applied based on *Calluna* cover ratios above 30%. Pixel colors correspond to the three remote sensing proxies *Calluna* coverage (red), stand structure (green; represented by the coefficient of variation between standard deviation and mean vegetation height) and co-occurring vegetation (blue). Reddish colors indicate mono *Calluna* stands. Green pixels feature a high structural diversity with low *Calluna* coverage and a low species index. This mainly applies to species poor zones influenced by grass encroachment. Less structured meadows that are home to many characteristic species are shown in blue. Although they lack sufficient *Calluna* coverage (<30%), they appear as fringes of *Calluna* heathland in the map due to the smoothing of the habitat mask. Apart from that, transitional zones between these three extremes can be found, appearing in yellow, cyan and pink. Areas where there is co-occurrence of high scores of the three layers appear in brighter colors. Thresholds from expert judgment were applied to the three quality layers in a rule-based procedure for classifying the conservation status per pixel (B). As *Calluna* coverage does not directly affect the conservation status classification, there might be cases where a shift between two classes can be seen in (B) that is not apparent in (A).

2012) might be worth to be examined as an alternative approach to estimate *Calluna* cover. However, we assume that the reported inaccuracies in the *Calluna* cover layer do not affect our classification result as the habitat mask summarizes zones with values above 30%. Differing from the approach of Schmidt et al. (2017b), who included *Calluna* cover into the quality assessment, we used the *Calluna* layer only for identifying the target habitat; habitat quality assessment was based on stand structure and co-occurring vegetation. This procedure is also more similar to what is described in the field guidelines.

The patterns represented by the species index were in agreement with what we expected from our field surveys. The depicted gradient from the species-rich calcareous

 

**Table 3.** Confusion matrix for assessing the fit of the conservation status map.

| Classified Data | Reference Data A | B | C | Total | User's accuracy |
|---|---|---|---|---|---|
| A | **49** | 10 | 9 | 68 | 0.72 |
| B | 2 | **22** | 5 | 28 | 0.79 |
| C | 6 | 6 | **49** | 61 | 0.80 |
| Total | 56 | 38 | 63 | 158 | |
| Producer's Accuracy | 0.88 | 0.58 | 0.78 | | |

Overall fit = 76%, Kappa = 0.64. Correct classifications are indicated by bold values.

grassland in the south of the study area to the degraded heathland in the north, where characteristic species only occur in small numbers, have also been observed in the previous work of Schmidt et al. (2017a) who mapped plant functional traits using airborne hyperspectral data. Although the index does not directly tell us whether adequate numbers of characteristic species are present, it provides information on the probability of their occurrence. A high species index indicates that the pixel is more likely to represent good habitat conditions in terms of co-occurring vegetation (Neumann et al. 2015). The species index was mainly useful for separating the habitat quality class 'A' from both other classes; classes 'B' and 'C' often featured similar scores. Stand structure, on the other hand, is crucial for separating 'B' and 'C'. It is apparent that there is often no gradual change from 'A' over 'B' to 'C', but a direct transition from 'A' to 'C'. For example, peripheral zones ('A') are directly neighboring overaged *Calluna* patches ('C').

Modeling the mean vegetation height delivered sound results. The corresponding quality layer allowed for identifying patches of old and tall *Calluna* plants as well as meadows of grasses and herbs in between. The standard deviation of the vegetation height was meaningful when used in combination with the mean height (as the coefficient of variation). Considered individually, the patterns were rather inconclusive. The combination of both height layers served as good indicator of the occurrence of *Calluna* growth phases.

## Transfer of the decision tree between calibration and test dataset

When applying the decision tree to the test dataset, the fit decreased to 73% (calibration reference = 76%). Studies that examined the transferability of decision tree classifications can rarely be found (Kalantar et al. 2017), and, if any, with respect to object-based analysis (Hofmann et al. 2011).

Modeling results of the quality layers were comparable between both remote sensing datasets. Here, we are in agreement with Feilhauer and Schmidtlein (2011) who reported minor deviations in model accuracies for different dates when examining similar habitats. Thus, short-term variation in image attributes due to slight changes in phenology probably had a minor impact on model performance. However, the optical-based species index representation most likely caused the switch from class 'C' to 'A' in larger patches in the upper part of Figure 6C. The deviation of one class is partly attributed to the poor performance of modeling the standard deviation of vegetation height for the transfer dataset.

To achieve more robust results, using multitemporal remote sensing information (Schuster et al. 2011; Buck et al. 2013; Zlinszky et al. 2015) and also the inclusion of multiseasonal data (Stenzel et al. 2014; Mack et al. 2016; Tarantino et al. 2016) could be examined in future work.

## Applicability to Natura 2000 monitoring scheme

The general modeling scheme shows the possibility to monitor heathland habitats based on the mapping guideline of the Habitats Directive and Copernicus products. However, since the Natura 2000 guidelines have not been developed considering the potential application of remote sensing data, the underlying parameters have to be slightly adapted for this use (Schmidt et al. 2017b).

From a conservationist's perspective, an object-based monitoring product might be preferred, since the reporting obligations often require clear patch-wise representations. However, converting pixel-wise to object-based results is connected to a loss of information due to generalization. Especially if extreme conservation status classes "favorable" and "bad" occur in close proximity, conditions might average in the intermediate class ("inadequate"). We believe that the focus on larger patches in current conservation guidelines is borne from a limitation of field-based approaches that need to refer to such units because continuous mapping in the field is difficult. In remote sensing-based approaches, the original spatial information can be reported without loss. Hence, although an aggregation of pixels is feasible we recommend to report the original pixel information when working with remote sensing data.

The overall fit of the result of 76% seems to indicate that there is room for improvement regarding the accuracy. Although this is certainly the case, one has to keep in mind the challenge of differentiating the conservation status of heathland, a task that is challenging even in a field-based study. According to Nieland et al. (2015), the reasons in mismatching field-based data and remote sensing data (besides methodological uncertainties and field-based mapping errors) are given in an improper

 

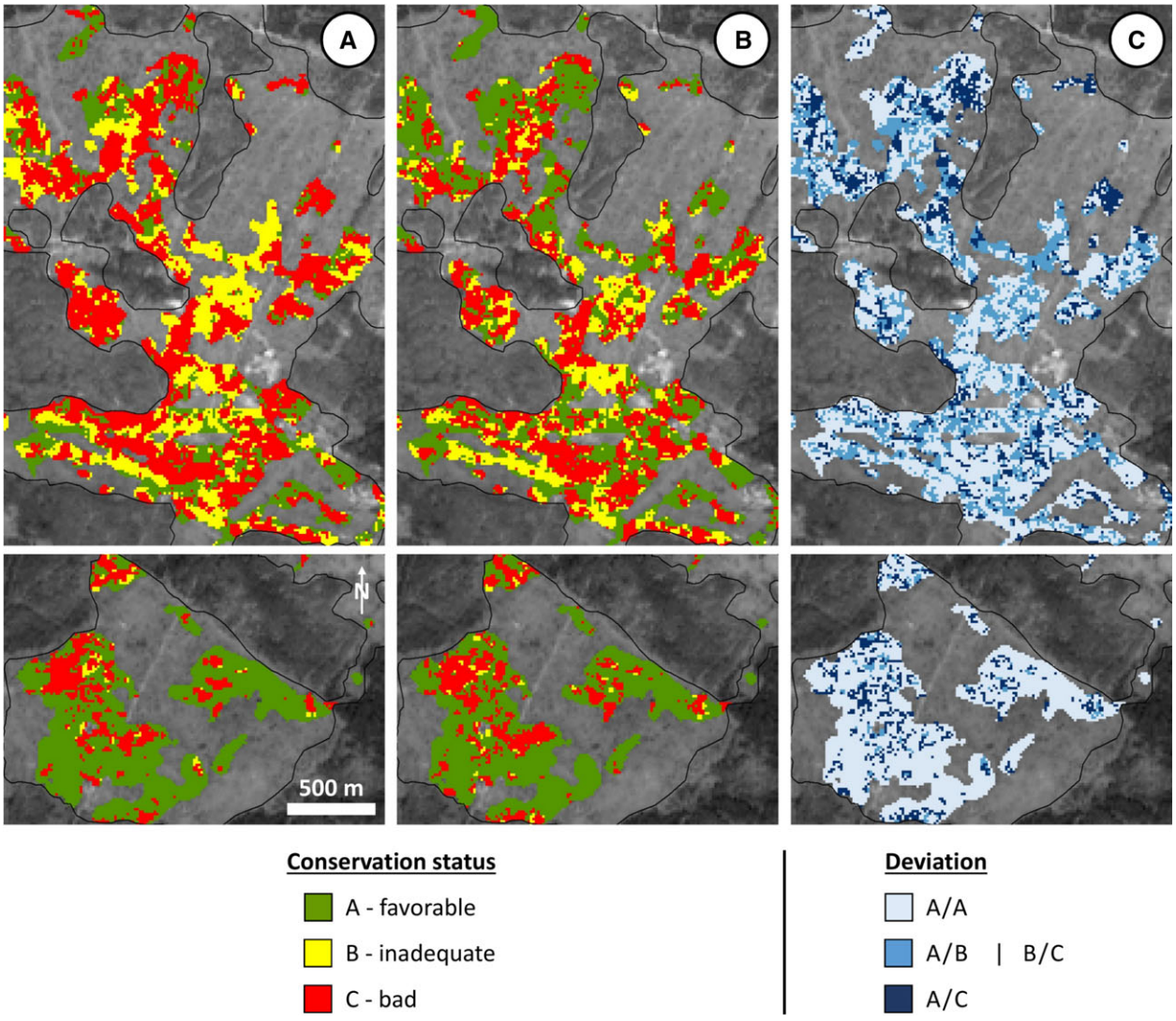


**Figure 6.** Conservation status map derived with the imagery from end of June / beginning of July (A; same as Fig. 5B) in comparison to the result from the dataset acquired around 3 weeks before (B). Deviation between both classification maps is shown in (C). An agreement of 60% between both results can be observed. Pixels with confusions between neighboring classes and extreme classes accounted for 23% and 17%, respectively. The habitat mask that was developed based on the calibration dataset from end of June was applied to all three maps to enhance comparability.

scale-match between field data and the resolution of the remotely sensed data (Small 2001). This can either produce smoothing effects or a high intra-class variation. Moreover, the field-based sampling strategies, even when intentionally aligned to the pixel-size of the sensor, do not fit perfectly to the pre-defined classes of the conservation status. This is less obvious, when we observe homogeneous classes with large spatial coverage. If the classes are spatially heterogeneous and spectrally similar, the task becomes more challenging. For these reasons, we assume the results as acceptable in terms of practical use for nature conservation purposes.

## Differences to related studies

Neumann et al. (2015) were able to map probabilities for both habitat types and conservation status classes by using a species-based ordination space. In this study, conservation status probabilities were not translated into discrete classes. However, this would be easy to realize by means of thresholds. The applicability of rule-based approaches has been demonstrated in other studies (e.g. Villa et al. 2015; Zlinszky et al. 2015). Haest et al. (2017) also applied knowledge-based rule sets for the quality assessment of Natura 2000 heathland habitats. In their

 

study, they suggested a patch-wise mapping of conservation status indicators, such as cover of encroaching grasses and trees. Subsequently, they assigned a status class ("favorable" or "unfavorable") to each indicator by applying exact thresholds from the field guidelines. They conclude that the application of thresholds upon habitat quality indicators represents a sound approximation of a rather complex assessment procedure that monitoring experts are accustomed to.

Similarly, Regan et al. (2004) formalized experts' decision process; in this case for conservation status assessments of single species. They explain that subjective assessments are often inconsistent and can hardly be repeated as they are influenced by, i.a., personal judgments and systematic biases (Tversky and Kahneman 1982; Plous 1993; Burgman 2001) and because the underlying reasoning is almost impossible to visualize (Keith and Ilowski 1999; Rush and Roy 2001). It is concluded that capturing the logical ordering of information, assumptions and reasoning, and transferring them into explicit rules allows for critical evaluation, refinement and reapplications. We consider our approach to be in agreement with this statement as thresholds to derive the conservation status can be revised after-the-fact, whereas this is hardly possible with field-based assessments.

The presented approach is in our perspective not restricted to Natura 2000 shrublands, but transferable to similar ecosystems characterized by a dominant shrub layer featuring few (or even one) dominant species. For example, Xian et al. (2015) also mapped single quality layers for heathlike landscapes in the USA, which they called "shrubland components", such as coverage of shrubs and herbaceous vegetation as well as vegetation height attributes. However, these products were in a much larger geographic extent and no quality assessment was included.

## Conclusion

In this study, we transferred rule-based field guidelines for quality assessment of dwarf shrub heathland to remote sensing-based quality layers (describing vegetation properties) using fused spaceborne Sentinel-1 SAR and multispectral Sentinel-2 remote sensing data.

The results indicate that the conservation status assessment by means of the three modeled quality layers does reflect field recorded habitat status information. According to our findings, co-occurring vegetation (besides the key species *Calluna*) is crucial for separating pixels representing a "favorable" conservation status from those representing an "inadequate" or "bad" conservation status, while the latter classes could be distinguished by means of the stand structure.

We recommend that future remote sensing-based mappings of habitat quality should more frequently consider including SAR data as it can deliver complementary information to optical imagery and is now freely and regularly available over the European Union's Copernicus system.

In our study, the strong orientation toward the field guidelines was thought to help bridging the often mentioned gap between applied conservation and the remote sensing community that mainly exists due to communication problems (Skidmore et al. 2015). Our approach could be used for a quick wall-to-wall characterization of a conservation area and thus provides a useful tool for site managers and decision makers. It still relies on field work (for model calibration) but the process of mapping is, in comparison to field work, less prone to biases and more capable to depict spatial mosaics.

We conclude that transferring operational field-based assessments into remote sensing approaches can be realized and is a promising option to avoid the development of completely new approaches. Existing assessment guidelines could be re-formulated in joint endeavors between field scientists and remote sensing experts in order to improve their compatibility with remotely sensed data. The essential biodiversity variables (EBVs; Pettorelli et al. 2016; Pereira et al. 2013) could play a key role in this respect.

## Acknowledgments

The study was supported by the German Federal Environmental Foundation (DBU, www.dbu.de). Access to the sites was enabled by the forestry district (Bundesforstbetrieb Mittelelbe). We thank B. Haest and an anonymous reviewer for the valuable comments which improved the manuscript.

## Conflicts of interest

The authors declare no conflicts of interest.

### References

Ausden, M. 2007. *Habitat management for conservation. A handbook of techniques*. Oxford University Press, Oxford, New York.

Bargiel, D. 2013. Capabilities of high resolution satellite radar for the detection of semi-natural habitat structures and grasslands in agricultural landscapes. *Ecol. Inform.* **13**, 9–16.

Barrett, B., C. Raab, F. Cawkwell, S. Green, H. Nagendra, and N. Horning. 2016. Upland vegetation mapping using Random Forests with optical and radar satellite data. *Remote. Sens. Ecol. Conserv.* **2**, 212–231.

Bock, M., G. Rossner, M. Wissen, K. Remm, T. Langanke, S. Lang, et al. 2005. Spatial indicators for nature conservation from European to local scale. *Ecol. Ind.* **5**, 322–338.

 

Buck, O., A. Klink, Elena García Millán V., Pakzad K., and A. Müterthies. 2013. Image analysis methods to monitor natura 2000 habitats at regional scales – the MS. MONINA state service example in schleswig-holstein, Germany. *Photogrammetrie - Fernerkundung - Geoinformation* **2013**, 415–426.

Burgman, M. A. 2001. Flaws in subjective assessments of ecological risks and means for correcting them. *Aust J Environ Manag* **8**, 219–226.

Carrasco, D., J. Díaz, A. Broquetas, R. Arbiol, M. Castillo, and V. Palà. 1997. Pp. 1789–1794 *Ascending-descending orbit combination SAR interferometry assessment*. Third ERS Symposium on Space at the Service of Our Environment, Florence, Italy.

Clasen, A., B. Somers, K. Pipkins, L. Tits, K. Segl, M. Brell, et al. 2015. Spectral unmixing of forest crown components at close range, airborne and simulated sentinel-2 and EnMAP spectral imaging scale. *Remote Sens.* **7**, 15361–15387.

Clevers, J., L. Kooistra, and M. van den Brande. 2017. Using sentinel-2 data for retrieving lai and leaf and canopy chlorophyll content of a potato crop. *Remote Sens.* **9**, 405.

Corbane, C., S. Lang, K. Pipkins, S. Alleaume, M. Deshayes, V. E. García Millán, et al. 2015. Remote sensing for mapping natural habitats and their conservation status – New opportunities and challenges. *Int. J. Appl. Earth Obs. Geoinf.* **37**, 7–16.

Crosetto, M. 2002. Calibration and validation of SAR interferometry for DEM generation. *ISPRS J. Photogramm. Remote Sens.* **57**, 213–227.

Delalieux, S., B. Somers, B. Haest, T. Spanhove, J. Vanden Borre, and C. A. Mücher. 2012. Heathland conservation status mapping through integration of hyperspectral mixture analysis and decision tree classifiers. *Remote Sens. Environ.* **126**, 222–231.

Delgado-Aguilar, M. J., F. E. Fassnacht, M. Peralvo, C. P. Gross, and C. B. Schmitt. 2017. Potential of TerraSAR-X and Sentinel 1 imagery to map deforested areas and derive degradation status in complex rain forests of Ecuador. *Int. Forest Rev.* **19**, 102–118.

Deo, R., C. Rossi, M. Eineder, T. Fritz, and Y. S. Rao. 2015. Framework for fusion of ascending and descending pass TanDEM-X raw DEMs. *IEEE J. Select. Topics Appl. Earth Obs. Remote Sens.* **8**, 3347–3355.

Duguay, Y., M. Bernier, E. Lévesque, and B. Tremblay. 2015. Potential of C and X band SAR for shrub growth monitoring in sub-arctic environments. *Remote Sens.* **7**, 9410–9430.

Dusseux, P., T. Corpetti, L. Hubert-Moy, and S. Corgne. 2014. Combined Use of multi-temporal optical and radar satellite images for grassland monitoring. *Remote Sens.* **6**, 6163–6182.

ESA (2016a). Sentinel-1 User Guide. Available at: https://earth.esa.int/web/sentinel/user-guides/sentinel-1-sar (last accessed: 6 February 2017).

ESA (2016b). Sentinel-2 User Guide. Available at:https://earth.esa.int/web/sentinel/user-guides/sentinel-2-msi.(last accessed: 6 February 2017)

ESA (2016c). SNAP. ESA Sentinel Application Platform.

Fassnacht, F. E., C. Neumann, M. Forster, H. Buddenbaum, A. Ghosh, A. Clasen, et al. 2014. Comparison of feature reduction algorithms for classifying tree species with hyperspectral data on three central european test sites. *IEEE J. Select. Topics Appl. Earth Obs. Remote Sens.* **7**, 2547–2561.

Feilhauer, H., and S. Schmidtlein. 2011. On variable relations between vegetation patterns and canopy reflectance. *Ecol Inform* **6**, 83–92.

Feilhauer, H., C. Dahlke, D. Doktor, A. Lausch, S. Schmidtlein, G. Schulz, et al. 2014. Mapping the local variability of Natura 2000 habitats with remote sensing. *Appl. Veg. Sci.* **17**, 765–779.

Felinks, B., S. Tischew, A. Lorenz, and S. Osterloh. 2012. Pflegemanagement von FFH-Offenlandlebensräumen in der Oranienbaumer Heide. Abschlussbericht für die Deutsche Bundesstiftung Umwelt (DBU). Available at: http://www.dbu.de/OPAC/ab/DBU-Abschlussbericht-AZ-25424_02.pdf.(last accessed 15 August 2016)

Foody, G. M. 2008. Harshness in image classification accuracy assessment. *Int. J. Remote Sens.* **29**, 3137–3158.

Förster, M., A. Frick, H. Walentowski, and B. Kleinschmit. 2008. Approaches to utilising QuickBird data for the monitoring of NATURA 2000 habitats. *Commun Ecol* **9**, 155–168.

Gernhardt, S., and R. Bamler. 2012. Deformation monitoring of single buildings using meter-resolution SAR data in PSI. *ISPRS J. Photogramm. Remote Sens.* **73**, 68–79.

Gimingham, C.H. 1972.*Ecology of heathlands*. Pp. 266. London: Chapman Hall xv, Illustrations, maps. Geog, 1.

Goering, D. J., Hao Chen, L. D. Hinzman, and D. L. Kane. 1995. Removal of terrain effects from SAR satellite imagery of arctic tundra. *IEEE Trans. Geosci. Remote Sens.* **33**, 185–194.

Haest, B., J. Vanden Borre, T. Spanhove, G. Thoonen, S. Delalieux, L. Kooistra, et al. 2017. Habitat mapping and quality assessment of NATURA 2000 heathland using airborne imaging spectroscopy. *Remote Sens.* **9**, 266.

Haralick, R.M., K. Shanmugam, and I. Dinstein. 1973. Textural features for image classification. *IEEE Transactions on Systems, Man, and Cybernetics SMC-3*,SMC-3: 610–621.

Hill, M. J., C. J. Ticehurst, Jong-Sen Lee, M. R. Grunes, G. E. Donald, and D. Henry. 2005. Integration of optical and radar classifications for mapping pasture type in Western Australia. *IEEE Trans. Geosci. Remote Sens.* **43**, 1665–1681.

Hofmann, P., T. Blaschke, and J. Strobl. 2011. Quantifying the robustness of fuzzy rule sets in object-based image analysis. *Int. J. Remote Sens.* **32**, 7359–7381.

Hong, S.-H., H.-O. Kim, S. Wdowinski, and E. Feliciano. 2015. Evaluation of polarimetric SAR decomposition for

 

classifying wetland vegetation types. *Remote Sens.* **7**, 8563–8585.

Immitzer, M., F. Vuolo, and C. Atzberger. 2016. First experience with sentinel-2 data for crop and tree species classifications in central Europe. *Remote Sens.* **8**, 166.

Kalantar, B., S. B. Mansor, M. I. Sameen, B. Pradhan, and H. Z. M. Shafri. 2017. Drone-based land-cover mapping using a fuzzy unordered rule induction algorithm integrated into object-based image analysis. *Int. J. Remote Sens.* **30**, 1–22.

Karatzoglou, A., S. Smola, K. Hornik, and A. Zeileis. 2004. kernlab – an S4 package for kernel methods in R. *J. Stat. Softw.* **11**, 1–20.

Keith, D., and M. Ilowski. 1999. *Epacris stuartii recovery plan 1996–2005*. Department of Primary Industries Water and Environment: Hobart.

Kepfer-Rojas, S., K. Verheyen, V. K. Johannsen, and I. K. Schmidt. 2015. Indirect effects of land-use legacies determine tree colonization patterns in abandoned heathland. *Appl. Veg. Sci.* **18**, 456–466.

Kuhn, M. (2016). caret: Classification and Regression Training. Available at: https://CRAN.R-project.org/package=caret(last accessed: 24 March 2017).

LAU 2010. Kartieranleitung Lebensraumtypen Sachsen-Anhalt - Teil Offenland. LAU - Landesamt für Umweltschutz Sachsen-Anhalt. Available at: http://www.lau.sachsen-anhalt.de/naturschutz/oeffentlichkeitsarbeit/publikationen/kartieranleitungen/ (last accessed: 1 July 2015).

Leutner, B. F., B. Reineking, J. Müller, M. Bachmann, C. Beierkuhnlein, S. Dech, et al. 2012. Modelling forest α-diversity and floristic composition — on the added value of lidar plus hyperspectral remote sensing. *Remote Sens.* **4**, 2818–2845.

Mack, B., R. Roscher, S. Stenzel, H. Feilhauer, S. Schmidtlein, and B. Waske. 2016. Mapping raised bogs with an iterative one-class classification approach. *ISPRS J. Photogramm. Remote Sens.* **120**, 53–64.

Millin-Chalabi, G., J. McMorrow, and C. Agnew. 2013. Detecting a moorland wildfire scar in the Peak district, UK, using synthetic aperture radar from ERS-2 and Envisat ASAR. *Int. J. Remote Sens.* **35**, 54–69.

Montesano, P. M., B. D. Cook, G. Sun, M. Simard, R. F. Nelson, K. J. Ranson, et al. 2013. Achieving accuracy requirements for forest biomass mapping. A spaceborne data fusion method for estimating forest biomass and LiDAR sampling error. *Remote Sens. Environ.* **130**, 153–170.

Mountrakis, G., J. Im, and C. Ogole. 2011. Support vector machines in remote sensing. A review. *ISPRS J. Photogramm. Remote Sens.* **66**, 247–259.

Nagler, P. L., C. Daughtry, and S. N. Goward. 2000. Plant litter and soil reflectance. *Remote Sens. Environ.* **71**, 207–215.

Neumann, C., G. Weiss, S. Schmidtlein, S. Itzerott, A. Lausch, D. Doktor, et al. 2015. Gradient-based assessment of habitat quality for spectral ecosystem monitoring. *Remote Sens.* **7**, 2871–2898.

Nieland, S., N. Moran, B. Kleinschmit, and M. Förster. 2015. An ontological system for interoperable spatial generalisation in biodiversity monitoring. *Comput. Geosci.* **84**, 86–95.

Pereira, H. M., S. Ferrier, M. Walters, G. N. Geller, R. H. G. Jongman, R. J. Scholes, et al. 2013. Ecology. Essential biodiversity variables. *Science (New York, N.Y.)* **339**, 277–278.

Peters, J., F. van Coillie, T. Westra, and R. de Wulf. 2011. Synergy of very high resolution optical and radar data for object-based olive grove mapping. *Int J Geogr Infor Sci* **25**, 971–989.

Pettorelli, N., M. Wegmann, A. Skidmore, S. Mücher, T. P. Dawson, M. Fernandez, et al. 2016. Framing the concept of satellite remote sensing essential biodiversity variables. Challenges and future directions. *Remote Sens. Ecol. Conserv.* **2**, 122–131.

Piñeiro, G., S. Perelman, J. P. Guerschman, and J. M. Paruelo. 2008. How to evaluate models. Observed vs. predicted or predicted vs. observed? *Ecol. Model.* **216**, 316–322.

Plous, S. 1993. *The psychology of judgment and decision making*. Mcgraw-Hill Book Company: New York.

R Development Core Team.2013. R. A language and environment for statistical computing.

Regan, T. J., L. L. Master, and G. A. Hammerson. 2004. Capturing expert knowledge for threatened species assessments. A case study using NatureServe conservation status ranks. *Acta. Oecologica.* **26**, 95–107.

Reiche, J., J. Verbesselt, D. Hoekman, and M. Herold. 2015. Fusing landsat and SAR time series to detect deforestation in the tropics. *Remote Sens. Environ.* **156**, 276–293.

Rodrigues, S. W. P., and P. W. M. Souza-Filho. 2011. Use of multi-sensor data to identify and map Tropical Coastal Wetlands in the Amazon of Northern Brazil. *Wetlands* **31**, 11–23.

Rush, C., and R. Roy. 2001. Expert judgement in cost estimating. Modelling the reasoning process. *Concurrent Eng.* **9**, 271–284.

Sansosti, E., R. Lanari, G. Fornaro, G. Franceschetti, M. Tesauro, G. Puglisi, et al. 1999. Digital elevation model generation using ascending and descending ERS-1/ERS-2 tandem data. *Int. J. Remote Sens.* **20**, 1527–1547.

Schmidt, J., F. E. Fassnacht, A. Lausch, and S. Schmidtlein. 2017a. Assessing the functional signature of heathland landscapes via hyperspectral remote sensing. *Ecol. Ind.* **73**, 505–512.

Schmidt, J., F. E. Fassnacht, C. Neff, A. Lausch, B. Kleinschmit, M. Förster, et al. 2017b. Adapting a Natura 2000 field guideline for a remote sensing-based assessment of heathland conservation status. *Int. J. Appl. Earth Obs. Geoinf.* **60**, 61–71.

 

Schmidtlein, S., L. Tichý, H. Feilhauer, and U. Faude. 2010. A brute-force approach to vegetation classification. *J. Veg. Sci.* **21**, 1162–1171.

Schuster, C., I. Ali, P. Lohmann, A. Frick, M. Förster, and B. Kleinschmit. 2011. Towards detecting swath events in TerraSAR-X time series to establish NATURA 2000 grassland habitat swath management as monitoring parameter. *Remote Sens.* **3**, 1308–1322.

Schuster, C., T. Schmidt, C. Conrad, B. Kleinschmit, and M. Förster. 2015. Grassland habitat mapping by intra-annual time series analysis – Comparison of RapidEye and TerraSAR-X satellite data. *Int. J. Appl. Earth Obs. Geoinf.* **34**, 25–34.

Skidmore, A. K., N. Pettorelli, N. C. Coops, G. N. Geller, M. Hansen, R. Lucas, et al. 2015. Environmental science: agree on biodiversity metrics to track from space. *Nature* **523**, 403–405.

Small, C. 2001. Estimation of urban vegetation abundance by spectral mixture analysis. *Int. J. Remote Sens.* **22**, 1305–1334.

Stenzel, S., H. Feilhauer, B. Mack, A. Metz, and S. Schmidtlein. 2014. Remote sensing of scattered Natura 2000 habitats using a one-class classifier. *Int. J. Appl. Earth Obs. Geoinf.* **33**, 211–217.

Tarantino, C., M. Adamo, R. Lucas, and P. Blonda. 2016. Detection of changes in semi-natural grasslands by cross correlation analysis with WorldView-2 images and new Landsat 8 data. *Remote Sens. Environ.* **175**, 65–72.

Tversky, A., and D Kahneman. 1982. Judgment under uncertainty: heuristics and biases. In D. Kahneman, P. Slovic, A Tversky (Eds.). *Judgment Under Uncertainty*. Cambridge University Press: Cambridge.

Ullmann, T., A. Schmitt, A. Roth, J. Duffe, S. Dech, H.-W. Hubberten, et al. 2014. Land cover characterization and classification of arctic tundra environments by means of polarized synthetic aperture X- and C-band radar (PolSAR) and landsat 8 multispectral imagery — Richards Island, Canada. *Remote Sens.* **6**, 8565–8593.

Vanden Borre, J., D. Paelinckx, C. A. Mücher, L. Kooistra, B. Haest, G. de Blust, et al. 2011. Integrating remote sensing in Natura 2000 habitat monitoring: prospects on the way forward. *J. Nat. Conserv.* **19**, 116–125.

Villa, P., D. Stroppiana, G. Fontanelli, R. Azar, and P. Brivio. 2015. In-season mapping of crop type with optical and X-band SAR data. A classification tree approach using synoptic seasonal features. *Remote Sens.* **7**, 12859–12886.

Watt, A. S. 1947. Pattern and process in the plant community. *J. Ecol.* **35**, 1.

Xian, G., C. Homer, M. Rigge, H. Shi, and D. Meyer. 2015. Characterization of shrubland ecosystem components as continuous fields in the northwest United States. *Remote Sens. Environ.* **168**, 286–300.

Zlinszky, A., B. Deák, A. Kania, A. Schroiff, and N. Pfeifer. 2015. Mapping natura 2000 habitat conservation status in a pannonic salt steppe with airborne laser scanning. *Remote Sens.* **7**, 2991–3019.

Zvoleff, A. 2015. glcm. Calculate textures from grey-level co-occurrence matrices GLCMs) in R. R package version 1.0.

## Supporting Information

Additional supporting information may be found online in the supporting information tab for this article.

**Data S1. Appendix**

**Table S1.** Variable importance of the single remote sensing bands for the SVM regression models.

 